scientific reports

Check for updates

OPEN

Serum lipid metabolites predict the efficacy of intravenous immune globulin therapy in patients with pediatric dilated cardiomyopathy

Zhiyuan Wang[1,2,3], Yanyan Xiao[3], Haichu Wen[4,5,6,7], Yifei Yang[3], Meng Yuan[4,5,6,7], Meng Jiao[1,2], Yan Gu[3], Mei Jin[1,2,3]✉ & Jie Du[4,5,6,7]✉

The response of pediatric dilated cardiomyopathy (PDCM) patients to intravenous immune globulin (IVIG) varies from cardiac functional recovery to heart transplantation and even death. IVIG therapy can significantly improve the left ventricular ejection fraction (LVEF) in some PDCM patients, but indicators for evaluating the response to IVIG therapy are lacking. Lipid metabolic disturbance is associated with changes in cardiac function, but no studies have examined the associations between lipidomics markers and the efficacy of IVIG. Discovery analyses were based on 322 targeted lipids in a retrospective cohort study. T tests, orthogonal–orthogonal projections to latent structures discriminant analysis (OPLS-DA) and random forest (RF) analysis were used to screen the candidate lipids. Associations of the candidate lipids were examined via Cox proportional hazards regression models. We subsequently developed a score for the candidate lipid metabolites, which was then used to classify children into two groups (0–3 and 4), and the survival curves of the two groups were drawn. There were 31 patients in the discovery set and 24 patients in the validation set. Adverse events which were defined as death, heart transplant, and rehospitalization for HF were observed in 23 patients (41.8%). After adjusting for age, LVEF, and the LV end-diastolic diameter z score, CE-16:1, PE36:4p, PE40:6p, and PE40:6p (22:6) were significantly associated with the occurrence of adverse events in the discovery set. The results were also consistent in the validation set, and the hazard ratios (HRs) were 2.638 (95% CI 1.042–6.683; $p = 0.041$), 0.549 (95% CI 0.340–0.886; $p = 0.014$), 0.271 (95% CI 0.109–0.672; $p = 0.005$), and 0.299 (95% CI 0.121–0.741; $p = 0.009$), respectively. We developed a score for these four lipid metabolites. When the score reached 4, adverse events were more likely to be observed in both sets. Serum lipid metabolites can be used to predict the efficacy of IVIG in children with DCM.

Keywords Pediatric dilated cardiomyopathy, Lipid metabolites, Intravenous immune globulin

Dilated cardiomyopathy (DCM) is the most common manifestation of cardiomyopathy in children and one of the main causes of heart failure (HF) and heart transplantation. Fewer than 40% of children who present with symptomatic HF survive for more than 5 years without cardiac transplantation[1,2]. Drug treatment for children with DCM mainly includes digitalis, diuretics and angiotensin converting enzymes. Previous studies have shown that the activation of inflammatory factors and the involvement of immune mechanisms are important pathways for the progression of HF[3,4]. Intravenous immune globulin (IVIG) has been shown to improve the left ventricular ejection fraction (LVEF) in children with DCM[5,6]. Currently, it is widely applied in many pediatric centers in China, but different research institutes have reported different therapeutic response rates, and biomarkers used to evaluate the therapeutic response to IVIG are still lacking[7]. In the past, we commonly used indicators, including high-sensitivity C-reactive protein and antiphospholipid antibodies. However, high-sensitivity C-reactive protein levels are significantly related to the occurrence of inflammatory responses,

[1]Department of Pediatric Heart Centre, Beijing Anzhen Hospital, Capital Medical University, Beijing, China. [2]Beijing Pediatric Heart Centre, Beijing, China. [3]Department of Cardiology, Beijing Children's Hospital, Capital Medical University, National Center for Children's Health (NCCH), No.56 Nanlishi Rd, Xicheng District, Beijing 10045, China. [4]Beijing Anzhen Hospital, Capital Medical University, Beijing, China. [5]Key Laboratory of Remodeling-Related Cardiovascular Diseases, Ministry of Education, Beijing, China. [6]Beijing Collaborative Innovation Centre for Cardiovascular Disorders, Beijing, China. [7]Beijing Institute of Heart, Lung and Blood Vessel Diseases, No. 2 Anzhen Rd, Chaoyang District, Beijing 100029, China. ✉email: jinmei_61@163.com; jiedu@ccmu.edu.cn

whereas antiphospholipid antibodies are closely associated with the presence of autoimmune diseases. Both measures obviously lack specificity[8]. Therefore, further studies are needed to identify biomarkers that can be used to predict the efficacy of IVIG in the treatment of children with DCM.

Microscopically, pediatric DCM (PDCM) is a cellular, genetic, proteomic and metabolite disorder. With the development of omics studies, we hope to be able to predict the efficacy of IVIG more accurately. The complex interactions between all omics layers and clinical risk factors are ultimately reflected as metabolic disturbances[9]. Metabolic disturbances can reflect changes in the pathological state of the body. Lipid metabolites are involved in a variety of biological processes, such as myocardial fibrosis and myocardial reverse remodeling[10], which provides a molecular basis for using lipid markers to predict the efficacy of IVIG and new ideas for understanding the pathogenesis of cardiovascular diseases and searching for possible biomarkers.

In our study, we used targeted metabolomics to analyze the clinical characteristics and prognosis of children with DCM who received IVIG therapy. We defined the composite outcome event as death, heart transplantation, or HF readmission. The treatment effect was evaluated by whether the composite outcome event occurred, and the patients were divided into an event group and a non-event group. Differential lipid metabolites between the two groups were screened, and they were used to construct a score to evaluate its ability to predict the improvement of adverse outcomes with IVIG therapy.

Materials and methods

The study was designed and carried out in accordance with the principles of the Declaration of Helsinki and was approved by the Beijing Anzhen Hospital Ethics Committee. Informed consent was obtained from all participants. More details are provided at ClinicalTrials.gov (NCT03076580).

Study population

This was a single-center retrospective study. The flow chart of the study is shown in Fig. 1. The study consists of a discovery set and a validation set. For the discovery set, 31 consecutive patients were enrolled in the study from March 2015 to December 2017 at Beijing Anzhen Hospital. The validation was set up from January 2018 to December 2019. Here, we used an absolute quantitative metabolomics platform to screen specific serum markers of adverse events.

The inclusion criteria were as follows: (1) aged 0–18 years; (2) disease duration < 6 months; (3) diagnosis of DCM, which was defined as an abnormal LVEF (< 50%), fractional shortening (FS, < 25%), and LV end-diastolic diameter (LVEDD) > 2 standard deviations (SDs) from normal according to nomograms (z scores > 2 SDs) corrected by body surface area (BSA) and age; (4) New York Heart Association (NYHA) functional classes II to IV (age ≥ 14) or modified Ross HF classification classes II to IV (age < 14); and (5) IVIG was infused monthly three times (1 g/kg*d, 2 days) and then every three months (1 g/kg*d, 2 days) for another three times.

The exclusion criteria were as follows: (1) other clinical conditions (e.g., rheumatoid arthritis, infection, etc.) that may increase cytokine levels; (2) ischemic cardiomyopathy (abnormal coronary arteries indicated by echocardiography or coronary angiography); (3) diagnosis of congenital heart disease via echocardiography; (4) cardiotoxic drugs; (5) hyperthyroidism; or (6) severe liver and kidney function damage.

Clinical data collection and follow-up

All clinical data, including patient sex, month, heart rate, cardiac medication, laboratory examination and echocardiography, were recorded when the patients were hospitalized for the first time. Patients were followed for at least one year after completing IVIG (2 g/kg) therapy. Follow-up records were obtained via echocardiography at outpatient clinics and telephone interviews. The adverse events included death, heart transplant, and rehospitalization for HF. We recorded whether and when an adverse event took place.

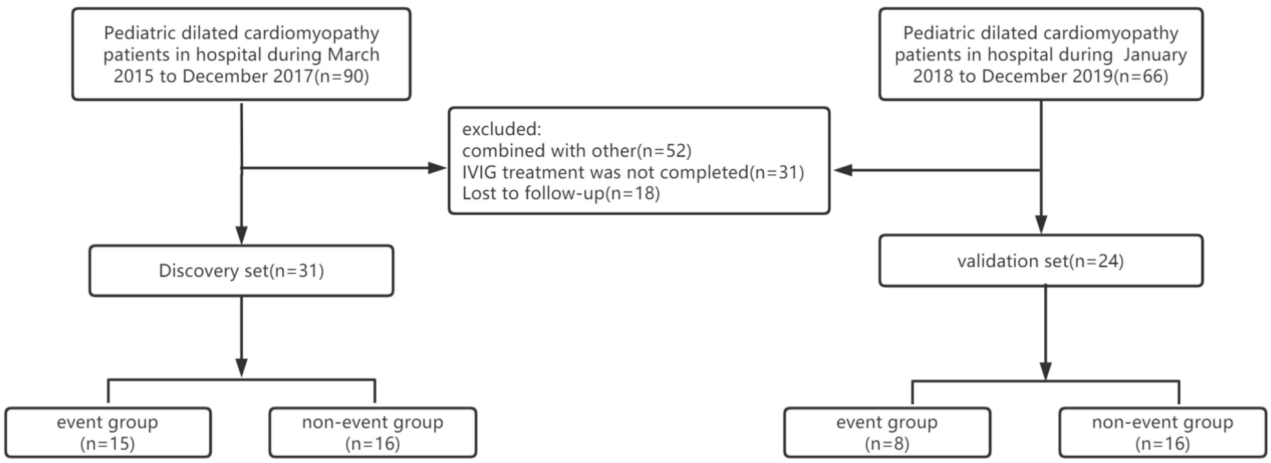

Fig. 1. Study flowchart. IVIG, intravenous immune globulin.

Blood sample collection and measurement of lipid metabolites

Blood samples were collected in the morning after at least 6–8 h of fasting and drawn into tubes with EDTA anticoagulant before IVIG therapy. The samples were subsequently centrifuged at 3000 rpm for 10 min in the clinical laboratory. The supernatant was quickly removed, and the samples were stored at − 80 °C. Lipid metabolites were extracted from the serum samples (20 µl) via an improved Bligh–Dyer extraction process (double extraction) in compliance with the appropriate internal standard. We scanned lipid metabolites on a UPLC system (Shimadzu, Kyoto, Japan) via multiple response monitoring (MRM) and analyzed them with a 6500 Plus QTRAP (Sciex, Framingham, MA, USA). The data miss rate (patient data and lipid metabolite data) was < 5%. The raw lipid metabolite concentrations were log-transformed and scaled (mean centered and divided by the SD) to maintain a symmetrical and comparable distribution. The false discovery rate (FDR) was used to control for multiple testing. We used machine learning to identify predictive biomarkers. The orthogonal-orthogonal projections to latent structures discriminant analysis (OPLS-DA) model (SIMCA 14.1) and random forest (RF) analysis were used to screen the candidate metabolites of adverse events.

Statistical analyses

Continuous variables are presented as medians and interquartile ranges and were compared via the Mann–Whitney U test. Categorical variables are shown as counts with percentages and were compared via the chi-square test or Fisher's exact test. Cox proportional hazards regression was used to calculate unadjusted and adjusted hazard ratios (HRs) after verifying the proportional hazards assumption. Spearman's correlation analysis revealed the relationships between candidate lipid metabolites and age, urea levels, the LVEDD z score, and the LVEF. Kaplan–Meier curves were generated, and differences between groups were assessed via the log-rank test. Analyses were performed via SPSS 23.0 (IBM, Chicago, IL, USA) and R version 3.4.0 (R Core Team, Vienna, Austria). All tests were two-sided, and a p value of < 0.05 was considered to indicate statistical significance.

Results

Baseline characteristics

The baseline characteristics of the discovery and validation sets are presented separately in Table 1. The baseline features of the discovery set and verification set are listed in Table 1. Baseline features were compared according to the occurrence of endpoint events. Adverse events were observed in 15 patients (48.4%), with a median follow-up time of 996 days (IQR: 155–1512 days). The median age of the PDCM patients was 20.0 months (IQR: 11.0–57.0), and 51.6% were male. There were significant differences in the LVEF and LVEDD before

	Discovery set			Validation set		
	Event group (n = 15)	Nonevent group (n = 16)	*P* value	Event group (n = 8)	Nonevent group (n = 16)	*P* value
Clinical characteristics						
Sex (male/female)	10/5	6/10	0.111	6/2	4/12	0.025
Age, month	17 (5, 57)	6 (4, 9)	0.013	118 (45, 175)	18 (9, 74)	0.018
Heart rate, bpm	129.20 ± 16.33	128.13 ± 17.70	0.862	106.75 ± 17.45	123.31 ± 15.50	0.027
Cardiac medication, n (%)						
Use of cardiotonic drug	15 (93)	16 (100)	–	8 (100)	16 (100)	–
Use of ACEIs	15 (100)	16 (100)	–	8 (100)	16 (100)	–
Use of beta-blockers	8 (53)	10 (63)	0.619	3 (38)	8 (50)	0.546
Use of diuretic agents	15 (100)	16 (100)	–	8 (100)	16 (100)	–
Use of IVIG	15 (100)	16 (100)	–	8 (100)	16 (100)	–
Laboratory results						
BNP, ng/L	424 (226, 1448)	94 (59, 242)	0.069	443 (196, 1307)	342 (62, 1100)	0.587
hs-CRP, mg/L	0.30 (0.11, 1.43)	0.22 (0.09, 0.55)	0.256	0.97 (0.43, 4.35)	0.18 (0.11, 0.32)	0.062
Urea, µmol/L	31.90 (21.08, 41.45)	25.00 (23.10, 27.70)	0.118	40.6 (36.75, 48.05)	23.85 (18.08, 30.85)	0.002
Triglycerides, mmol/L	0.73 (0.47, 0.99)	0.78 (0.57, 1.20)	0.715	1.18 (0.68, 1.48)	0.86 (0.67, 1.35)	0.384
Totle cholesterol, mmol/L	4.11 (3.33, 4.57)	3.85 (3.36, 4.02)	0.993	4.33 (3.49, 4.73)	4.65 (3.81, 5.13)	0.369
LDL cholesterol, mmol/L	2.18 (1.76, 2.90)	2.09 (1.74, 2.51)	0.550	2.87 (2.55, 3.31)	2.75 (2.15, 3.05)	0.789
Echocardiography-first						
LVEDD z score	7.19 ± 2.24	4.74 ± 1.84	0.009	5.40 ± 1.77	6.80 ± 2.76	0.147
LVEF/%	35.20 ± 7.06	42.56 ± 7.57	0.003	29.81 ± 9.63	35.75 ± 7.87	0.157
Echocardiography-following						
LVEDD z score	4.18 ± 1.53	2.80 ± 1.58	0.06	5.76 ± 3.32	3.87 ± 1.02	0.07
LVEF/%	42.22 ± 5.32	54.43 ± 12.41	0.01	36.00 ± 16.78	54.30 ± 10.95	0.01

Table 1. Baseline characteristics of pediatric dilated cardiomyopathy (PDCM) patients in the discovery set and validation set. *BNP* brain natriuretic peptide, *LDL* low-density lipoprotein, *LVEDD* left ventricular end-diastolic diameter, *LVEF* left ventricular ejection fraction. Categorical variables are reported as count (%) and continuous variables as median (IQR).

treatment between the two groups, but there were no significant differences in the laboratory results. The use of cardiac drugs was similar between the two groups. Fifteen patients (48.4%) experienced adverse events in the discovery set, including 4 children who died from cardiac causes and 11 children with HF readmission. Eight patients (33.3%) had endpoint events in the validation set, including 3 children who died from cardiac causes, 1 child who received heart transplantation, and 4 children with HF readmission. The median follow-up time was 133 days (IQR: 37–227). The median age of the PDCM patients was 30 (16–111) months, and 25% were male.

Screening of candidate lipid metabolites

In the discovery set, 32 lipid metabolites were significantly associated with the occurrence of adverse events ($p < 0.05$), as shown in Table 2. Then, we showed the important features selected via a volcano plot with a fold change threshold (x) of 1.2 and a t test threshold (y) of 0.05 (Fig. 2). Red represents upregulated metabolites (15 in total), blue represents downregulated metabolites (17 in total), and gray represents nondifferentiated metabolites.

The OPLS-DA model was used to screen candidate features (Fig. 3). The lipid metabolites with VIP > 1 are shown in Fig. 3. The event and nonevent groups were significantly different. We then used RF to define the differences in the lipid metabolic profiles of the two groups. Thus, the top 15 lipid metabolites were selected (Fig. 4). Finally, through the intersection of features selected by the three methods described above, we identified four lipid metabolites, namely, CE-16:1, PE36:4p, PE40:4p, PE40:6p, and PE40:6p (22:6).

Serum lipid metabolite scores and prediction of the efficacy of intravenous immune globulin therapy

In the discovery set, after adjusting for age, LVEF, and the LVEDD z score, CE-16:1, PE36:4p, PE40:6p, and PE40:6p (22:6) were significantly associated with the occurrence of adverse events. The HRs were 2.638 (95% CI 1.042–6.683; $p = 0.041$), 0.549 (95% CI 0.340–0.886; $p = 0.014$), 0.271 (95% CI 0.109–0.672; $p = 0.005$), and 0.299 (95% CI 0.121–0.741; $p = 0.009$). We subsequently developed a score for these four lipid metabolites. If the

	Compounds	V	*p* value	−log10 (p)	FDR
1	PE40:4p	44	0.0020067	2.6975	0.29144
2	GluCer d18:0/24:1	44	0.0020067	2.6975	0.29144
3	PE40:5p	46	0.0027153	2.5662	0.29144
4	GluCer d18:1/16:0	46	0.0036651	2.4359	0.29504
5	PG36:2 (18:0)	54	0.0082127	2.0855	0.44876
6	TAG50:1 (16:0)	181	0.015209	1.8179	0.44876
7	TAG50:1 (18:1)	181.5	0.015888	1.7989	0.44876
8	PE40:6p	59	0.01677	1.7755	0.44876
9	CE-16:1	180.5	0.017695	1.7522	0.44876
10	TAG50:0 (18:0)	179.5	0.019654	1.7065	0.44876
11	PE38:7	60.5	0.019667	1.7063	0.44876
12	PE36:4p	61	0.020742	1.6832	0.44876
13	TAG46:1 (16:1)	178	0.021463	1.6683	0.44876
14	PE40:6 (20:4)	61.5	0.021855	1.6605	0.44876
15	TAG46:2 (16:1)	177	0.02551	1.5933	0.44876
16	PE40:6p (22:6)	63	0.02551	1.5933	0.44876
17	DAG36:1 (18:1/18:0)	176	0.028232	1.5493	0.44876
18	PE38:5p (20:4)	64	0.028232	1.5493	0.44876
19	PE40:4p (20:4)	64	0.028232	1.5493	0.44876
20	PE38:6p	65	0.029751	1.5265	0.44876
21	TAG52:0 (18:0)	174.5	0.032781	1.4844	0.44876
22	TAG48:0 (16:0)	173	0.036637	1.4361	0.44876
23	TAG56:5 (18:2)	67	0.036637	1.4361	0.44876
24	GluCer d18:1/22:0	67	0.037944	1.4209	0.44876
25	LPA16:1	172.5	0.039813	1.4	0.44876
26	TAG56:5 (20:2)	68	0.040543	1.3921	0.44876
27	TAG48:1 (16:0)	172	0.041758	1.3793	0.44876
28	TAG48:1 (16:1)	171.5	0.043784	1.3587	0.44876
29	TAG50:2 (16:1)	171.5	0.043784	1.3587	0.44876
30	LPE18:2	171.5	0.043784	1.3587	0.44876
31	DAG34:1 (16:0/18:1)	170	0.049381	1.3064	0.44876
32	SM18:1/24:0	70	0.049381	1.3064	0.44876

Table 2. Important features identified by t tests. V, the degree of freedom.

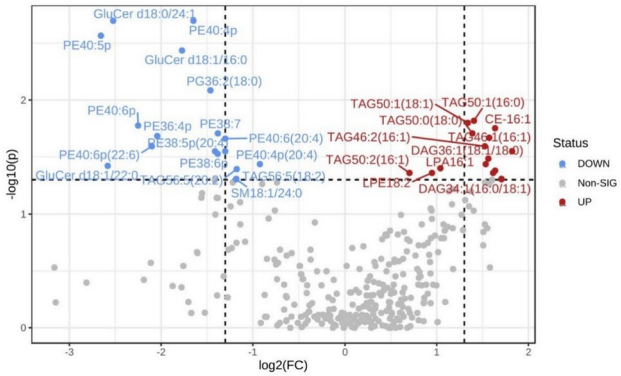

Fig. 2. The important features selected by the volcano plot with a fold change threshold (x) of 1.2 and a t test threshold (y) of 0.05. The red circles represent features above the threshold. Note that both the fold changes and p values are log transformed. The further its position is from (0,0), the more significant the feature is.

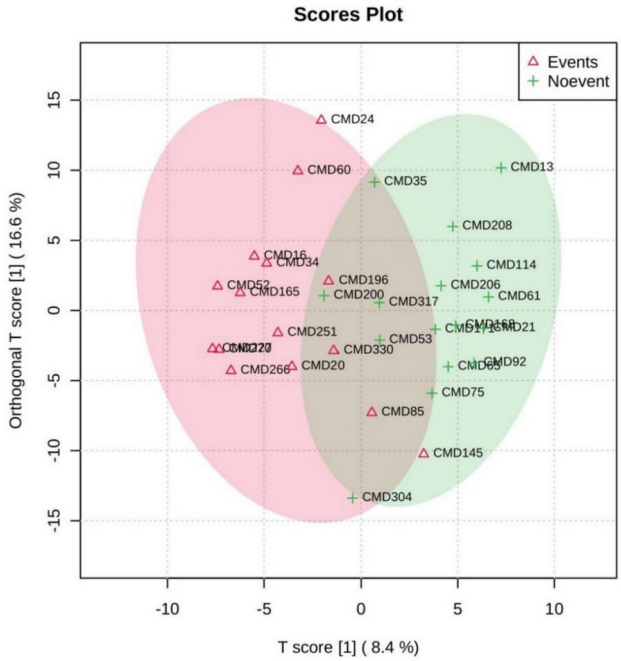

Fig. 3. OPLS-DA score plot of all metabolite features. Each dot represents a lipid metabolite; the event group is shown in pink, and the nonevent group is shown in green. The abscissa represents the score value of the predicted component, and the difference between the groups can be seen in the abscissa direction. The ordinate represents the orthogonal component score values, and the ordinate direction represents the gap within the group.

CE-16:1 score was above the median, one point was given. If PE36:4p, PE40:6p and PE40:6p (22:6) were below the median, one point was given. Finally, the total lipid metabolite score was calculated, ranging from 0 to 4. The participants were divided into two groups according to their scores, namely, group 0–3 and group 4. The survival curves of the two groups were drawn (Fig. 5). When the score reached 4, adverse events were more likely to be observed in both sets. The difference in the KM curves may be due to the smaller cohorts and lower event rates, but the lipid score showed a consistent stratification effect in both datasets. Our results indicated that four LysoPAs were independent predictors of the efficacy of IVIG therapy.

Discussion

The prognosis for PDCM varies widely and includes death, heart transplantation and improved left ventricular function[11]. At present, owing to its immunomodulatory and anti-inflammatory effects, IVIG is used to treat patients with PDCM in clinical practice, but there is still a lack of serum markers that can predict the effectiveness of IVIG therapy to achieve accurate treatment. Metabolomics studies the interaction and characteristics of small-molecule metabolites under given conditions and is an important component of lipid metabolites. In contrast

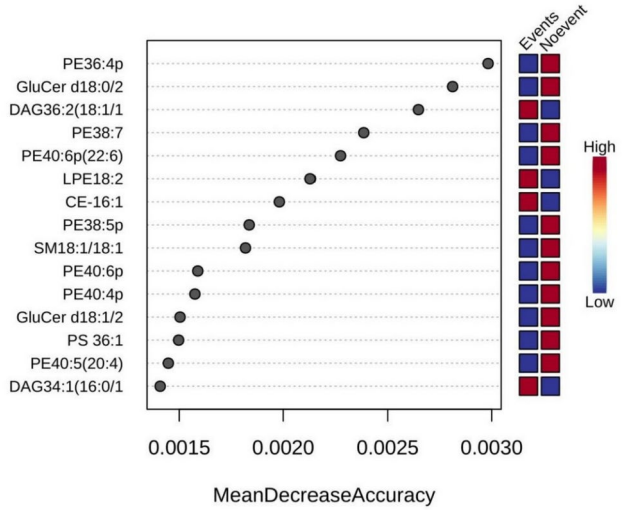

Fig. 4. Significant features identified by random forest. The features are ranked by the mean decrease in classification accuracy when they are permuted.

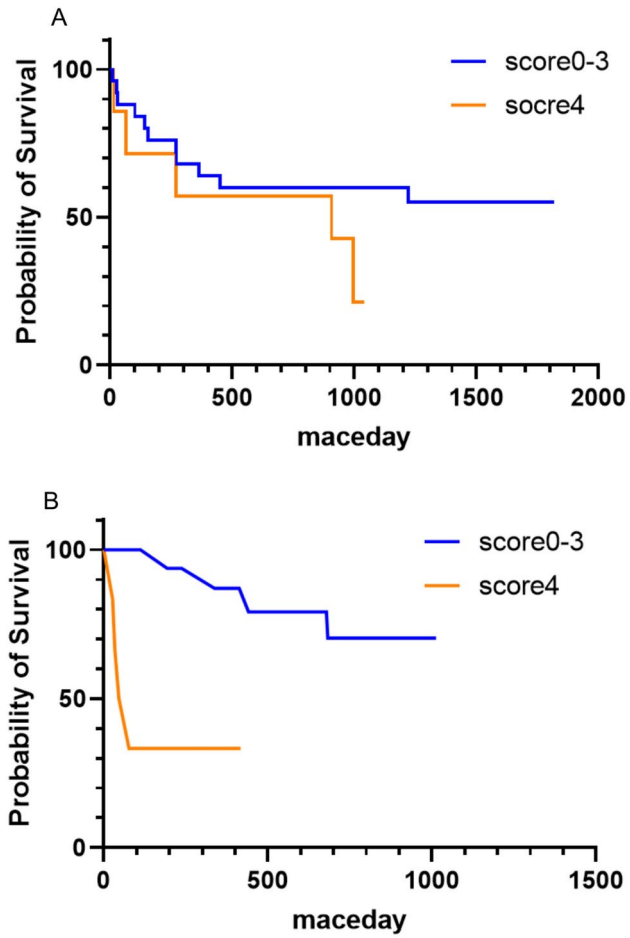

Fig. 5. Kaplan–Meier cumulative event curve of the serum lipid metabolite score for predicting the efficacy of intravenous immune globulin therapy in the discovery set (**A**) and validation set (**B**).

to genome, transcriptome and protein research, metabolomics studies the end products of cellular activities and is considered the most stable. In this study, lipid metabolites were analyzed via nontargeted metabolomics in the PDCM cohort, and their correlation with cardiovascular adverse events was analyzed. CE-16:1, PE36:4p, PE40:6p, and PE40:6p (22:6) may predict the therapeutic effect of IVIG. Furthermore, we established a lipid score composed of differential lipids that independently predicted the effectiveness of IVIG therapy.

Although 30–50% of children are classified as having familial DCM because of genetic factors[12], several studies have shown that changes in energy metabolism are important factors in the development and progression of cardiomyopathy. In a normal body, 60% to 90% of the energy supply of the heart comes from the oxidation of fatty acids, and most of the rest comes from the oxidation of glucose, with a small amount coming from ketone bodies, amino acids, etc. Impaired fatty acid oxidation can lead to DCM[13]. Fatty acids of different chain lengths are substrates for cellular oxidative phosphorylation to produce energy. Owing to the lack of malonyl CoA (CoA) decarboxylase in some children, malonyl CoA cannot be converted into acetyl CoA and carbon dioxide. These children present with an enlarged heart and develop acute HF or multisystem failure in the neonatal stage[14,15]. Moreover, sphingolipid metabolism disorders can also lead to the development of heart disease. Sphingolipid diseases are characterized by lysosomal storage disorders characterized by inadequate enzyme activity due to abnormal sphingolipid metabolism, such as Anderson–Fabry disease. This type of dilated heart disease manifests as progressive myocardial hypertrophy in the early stages, which may later lead to ventricular dilation and decreased systolic function[16]. In addition, adverse changes in the structure and function of cardiomyocytes in the enlarged heart, such as irregular cardiomyocyte hypertrophy, fibrosis, and cardiomyocyte necrosis, lead to ventricular remodeling and ultimately the development of HF[17]. Lipid metabolism may also be involved in the above pathological processes. Zhang L et al. reported that abnormal expression of lipids could affect substrate utilization by cardiomyocytes[18]. The OMEGA-REMODEL randomized controlled study demonstrated that ω3-PUFAs reduced the left ventricular systolic volume index and myocardial fibrosis levels[19]. Moreover, previous studies have shown that ganglioside 1 (GM1) can protect rat cardiac fibroblasts from C2-ceramide-induced myocardial apoptosis[20].

A reduction in fatty acid oxidation can lead to insufficient mitochondrial energy production. ATP binding and dissociation of myosin are essential for maintaining stable contraction of cardiomyocytes. ATP production is reduced, resulting in decreased myocardial contractility. Moreover, due to insufficient concentrations or incomplete functions of some enzymes in the process of fatty acid oxidation, intermediate metabolites such as lipids and long-chain acylcarnitines cannot be converted to final products or transport obstacles, and intracellular metabolic waste accumulates, thus leading to cell damage[21–23]. The above two pathways may be the possible mechanisms of fatty acid metabolism in children with DCM. We found that CE-16:1, PE36:4p, PE40:6p, and PE40:6p (22:6) were significantly correlated with the effectiveness of propyl bulb therapy in children with cardiopathy. Previous studies have shown that the mean increase in the c-statistic/AUC for congestive HF (CHF) prediction studies was 0.0752 (SE 0.0460) when metabolite biomarkers were added to the baseline biomarker prediction model. Two types of lipids were found in this study: cholesterol esters (CEs) and phosphatidylethanolamine (PE). CEs and natural cholesterol are the most common lipids. Most CEs enter the circulation as a component of lipoprotein (LDL, VLDL, HDL)[9]. In a population-based lipidomics study, monounsaturated CE-16:1 was found to be positively associated with cardiovascular disease risk[24]. PE is a lipid chaperone that is synthesized mainly in the endoplasmic reticulum and mitochondria[24]. Under pathological conditions, the balance between saturated lipids and unsaturated lipids is affected mainly through endoplasmic reticulum stress and ferroptosis, resulting in a decrease in cell membrane stability and, ultimately, cell apoptosis. Previous animal studies have also demonstrated significant changes in cardiac lipids in models of stress-induced HF[25,26].

Given the widespread application of IVIG therapy in children with DCM, identifying a predictor of therapeutic effectiveness is important. In our study, we screened CE 16:1, PE 36:4p, PE 40:6p and PE 40:6p (22:6) from 322 lipid metabolites, and it is likely that they will play major biological roles. On this basis, we constructed a lipid score to further improve the prediction efficiency. On the one hand, we are taking a step forward in distinguishing children with different outcomes; on the other hand, we also provide information for identifying potential therapeutic targets that can be cost-effective and avoid overtreatment.

However, there are obvious limitations to this study. First, owing to the existence of biodiversity, measurement variability, sampling error and other reasons, metabolomic test results may have errors, and changes in the medication history, dietary pattern and environmental exposure of children may affect metabolomic sampling. Thus, it is necessary to standardize data collection methods to improve sampling accuracy. Second, the coverage of lipid metabolites is incomplete. We used a targeted measurement that examined 322 different lipids, but the coverage was still incomplete. Third, although we utilized data and samples from two large cardiovascular centers, owing to limitations of incidence and short sample collection time, only 55 samples were included in the case group; therefore, increasing the sample size and adding an external cohort to verify the results of this study are necessary.

Conclusion

In conclusion, we revealed the relationship between the serum lipidomics profiles and outcomes in patients with PDCM who were treated with IVIG. The serum lipid metabolites CE-16:1, PE36:4p, PE40:6p, and PE40:6p (22:6) can be used to predict the efficacy of IVIG in patients with PDCM. When CE-16:1 was lower and PE36:4p, PE40:6p, and PE40:6p (22:6) were higher, IVIG therapy was more effective. When the score reached 4, adverse events were more likely to be observed in our study.

Data availability

The datasets used and/or analysed during the current study available from the corresponding author on reasonable request.

Received: 19 June 2024; Accepted: 26 March 2025
Published online: 12 May 2025

References

1. Pahl, E. et al. Incidence of and risk factors for sudden cardiac death in children with dilated cardiomyopathy: A report from the Pediatric Cardiomyopathy Registry. *J. Am. Coll. Cardiol.* **59**(6), 607–615. https://doi.org/10.1016/j.jacc.2011.10.878 (2012).
2. Singh, T. P. et al. Association of left ventricular dilation at listing for heart transplant with postlisting and early posttransplant mortality in children with dilated cardiomyopathy. *Circ. Heart Fail.* **2**(6), 591–598. https://doi.org/10.1161/CIRCHEARTFAILURE.108.839001 (2009).
3. Wu, J., Dong, E., Zhang, Y. & Xiao, H. The role of the inflammasome in heart failure. *Front Physiol.* **12**, 709703. https://doi.org/10.3389/fphys.2021.709703 (2021).
4. Ameling, S. et al. Myocardial gene expression profiles and cardiodepressant autoantibodies predict response of patients with dilated cardiomyopathy to immunoadsorption therapy. *Eur. Heart J.* **34**(9), 666–675. https://doi.org/10.1093/eurheartj/ehs330 (2013).
5. Heidendael, J. et al. Intravenous immunoglobulins in children with new onset dilated cardiomyopathy. *Cardiol. Young* **28**(1), 46–54. https://doi.org/10.1017/S1047951117001561 (2018).
6. Gullestad, L. et al. Immunomodulating therapy with intravenous immunoglobulin in patients with chronic heart failure. *Circulation* **103**(2), 220–225. https://doi.org/10.1161/01.cir.103.2.220 (2001).
7. Aukrust, P. et al. The role of intravenous immunoglobulin in the treatment of chronic heart failure. *Int. J. Cardiol.* **112**(1), 40–45. https://doi.org/10.1016/j.ijcard.2006.05.015 (2006).
8. Ribeiro, É. C. T., Sangali, T. D., Clausell, N. O., Perry, I. S. & Souza, G. C. C-reactive protein and frailty in heart failure. *Am. J. Cardiol.* **166**, 65–71. https://doi.org/10.1016/j.amjcard.2021.11.018 (2022).
9. McGranaghan, P. et al. Lipid metabolite biomarkers in cardiovascular disease: Discovery and biomechanism translation from human studies. *Metabolites* **11**(9), 621. https://doi.org/10.3390/metabo11090621 (2021).
10. Ampong, I. Metabolic and metabolomics insights into dilated cardiomyopathy. *Ann. Nutr. Metab.* **78**(3), 147–155. https://doi.org/10.1159/000524722 (2022).
11. Jefferies, J. L. & Towbin, J. A. Dilated cardiomyopathy. *Lancet* **375**(9716), 752–762. https://doi.org/10.1016/S0140-6736(09)62023-7 (2010).
12. Lipshultz, S. E. et al. Cardiomyopathy in children: classification and diagnosis: A scientific statement from the American Heart Association. *Circulation* **140**(1), e9–e68. https://doi.org/10.1161/CIR.0000000000000682 (2019).
13. Magoulas, P. L. & El-Hattab, A. W. Systemic primary carnitine deficiency: An overview of clinical manifestations, diagnosis, and management. *Orphanet. J. Rare Dis.* **7**, 68. https://doi.org/10.1186/1750-1172-7-68 (2012).
14. Wang, S. M., Hou, J. W. & Lin, J. L. A retrospective epidemiological and etiological study of metabolic disorders in children with cardiomyopathies. *Acta Paediatr. Taiwan.* **47**(2), 83–87 (2006).
15. Bonnet, D. et al. Efficiency of metabolic screening in childhood cardiomyopathies. *Eur. Heart J.* **19**(5), 790–793. https://doi.org/10.1053/euhj.1997.0818 (1998).
16. Takenaka, T. et al. Terminal stage cardiac findings in patients with cardiac Fabry disease: An electrocardiographic, echocardiographic, and autopsy study. *J. Cardiol.* **51**(1), 50–59. https://doi.org/10.1016/j.jjcc.2007.12.001 (2008).
17. Weintraub, R. G. & Alexander, P. M. A. Outcomes in pediatric dilated cardiomyopathy: Quo Vadis?. *J. Am. Coll. Cardiol.* **70**(21), 2674–2676. https://doi.org/10.1016/j.jacc.2017.09.1100 (2017).
18. Zhang, L., Wang, G. C., Ma, L. & Zu, N. Cardiac involvement in adult polymyositis or dermatomyositis: A systematic review. *Clin. Cardiol.* **35**(11), 686–691. https://doi.org/10.1002/clc.22026 (2012).
19. Heydari, B. et al. Effect of omega-3 acid ethyl esters on left ventricular remodeling after acute myocardial infarction: The OMEGA-REMODEL Randomized Clinical Trial. *Circulation* **134**(5), 378–391. https://doi.org/10.1161/CIRCULATIONAHA.115.019949 (2016).
20. Cavallini, L., Venerando, R., Miotto, G. & Alexandre, A. Ganglioside GM1 protection from apoptosis of rat heart fibroblasts. *Arch. Biochem. Biophys.* **370**(2), 156–162. https://doi.org/10.1006/abbi.1999.1378 (1999).
21. Lopaschuk, G. D., Ussher, J. R., Folmes, C. D., Jaswal, J. S. & Stanley, W. C. Myocardial fatty acid metabolism in health and disease. *Physiol Rev.* **90**(1), 207–258. https://doi.org/10.1152/physrev.00015.2009 (2010).
22. Das, A. M., Steuerwald, U. & Illsinger, S. Inborn errors of energy metabolism associated with myopathies. *J. Biomed. Biotechnol.* **2010**, 340849. https://doi.org/10.1155/2010/340849 (2010).
23. Cox, G. F. Diagnostic approaches to pediatric cardiomyopathy of metabolic genetic etiologies and their relation to therapy. *Prog. Pediatr. Cardiol.* **24**(1), 15–25. https://doi.org/10.1016/j.ppedcard.2007.08.013 (2007).
24. Vance, J. E. Phospholipid synthesis and transport in mammalian cells. *Traffic* **16**(1), 1–18. https://doi.org/10.1111/tra.12230 (2015).
25. Patel, D. & Witt, S. N. Ethanolamine and phosphatidylethanolamine: Partners in health and disease. *Oxid. Med. Cell. Longev.* **2017**, 4829180. https://doi.org/10.1155/2017/4829180 (2017).
26. Salatzki, J. et al. Adipose tissue ATGL modifies the cardiac lipidome in pressure-overload-induced left ventricular failure. *PLoS Genet.* **14**(1), e1007171. https://doi.org/10.1371/journal.pgen.1007171 (2018).

Acknowledgements

We thank Matt A., Senior Editor, from Springer nature author service for editing the English text of a draft of this manuscript.

Author contributions

Z.W (First Author): Conceptualization, Methodology, Investigation, Writing—Original Draft; Y.X: Data Curation, Writing—Original Draft; H.W: Software, Visualization, Investigation, Formal Analysis; Y.Y: Resources, Supervision, Validation, Writing—Review & Editing; M.Y: Software, Validation; M.J and Y.G: Resources, Writing—Review & Editing; M.J and J.D(Corresponding Author):Conceptualization, Funding Acquisition, Resources, Supervision, Writing—Review & Editing.

Funding
This study was funded by the National Key R&D Program of China (Grant No. 2021YFA0805100) and the National Natural Science Foundation of China (Grant Nos. 82241206 and 82070413).

Competing interests
The authors declare no competing interests.

Additional information
Correspondence and requests for materials should be addressed to M.J. or J.D.

Reprints and permissions information is available at www.nature.com/reprints.

Publisher's note Springer Nature remains neutral with regard to jurisdictional claims in published maps and institutional affiliations.